2007 IEEE International Conference on
Robotics and Automation
Roma, Italy, 10-14 April 2007



# Parallel Mechanisms of the Multipteron Family: Kinematic Architectures and Benchmarking

Clément M. Gosselin, Mehdi Tale Masouleh, Vincent Duchaine, Pierre-Luc Richard, Simon Foucault and Xianwen Kong

***Abstract*— This paper is a contribution to an invited session on the benchmarking of parallel mechanisms. The aim of the session is to compare different existing designs and prototypes of parallel mechanisms using a common set of benchmarking criteria. First, the kinematic architectures of parallel mechanisms of the multipteron family are presented. In addition to the Tripteron and the Quadrupteron, the Pentapteron, a five-degree-of-freedom (dof) parallel mechanism is introduced. Then, the benchmarking criteria are applied to the prototypes of the Tripteron (3-dof) and the Quadrupteron (4-dof) prototypes. Although the Tripteron and Quadrupteron parallel mechanisms have been presented elsewhere, their properties, highlighted by the benchmarking analysis presented here are revealed for the first time.**

## I. INTRODUCTION

Although hexapods, six-dof (degree-of-freedom) parallel mechanisms, can be used as versatile robots and machine tools, their complexity is a major deterrent to their widespread in industry. Indeed, in several manipulation and manufacturing applications, simpler low-cost 3-dof and 4-dof mechanisms are sufficient. In the machine tool industry, for instance, manufacturers have introduced several 3-dof parallel machines over the last decade. Most of these machines are based on the Delta robot [1], a translational 3-dof parallel mechanism. Examples of such machines include the Triaglide built by Mikron, the Quickstep by Krause & Mauser, the VerticalLine V100 by INDEX-Werke, the Urane SX by Comau, and the PEGASUS by Reichenbacher.

In robotics, 3-dof and 4-dof arms represent a large proportion of all the robots in use. In particular, the Cartesian robots (translational robots) and the SCARA architecture [2], which can produce the 4-dof Schönflies motions (also called SCARA motions), are very widely used. Therefore, researchers working on parallel mechanisms have proposed many architectures capable of producing these simple motion patterns.

Translational parallel mechanisms have been invented in great numbers, ever since Clavel proposed his Delta robot [3]. Examples include the typical design with three universal-revolute-universal-joint legs or its slight variations [4], [5], [6], or designs including parallelograms [7], other than the obvious variations of the Delta robot. Several systematic approaches were also proposed for the type synthesis of translational parallel mechanisms, such as methods based on displacement group theory [8], [9] and methods based on screw algebra or screw theory [10], [11].[1] The Tripteron [13], the first robot of the family studied in this paper, arose from the type synthesis presented in the latter reference.

One of the earliest examples of parallel mechanism implementing the Shönflies motions was a variation of the Delta robot [3]. Later, Angeles et al. [14] proposed an architecture based on parallelogram linkages, as well as an architecture based on two legs [15], which can both be thought of as hybrid architectures. Concurrently, the H4 robot, a fully parallel Shönflies motion generator, was introduced [16]. Also, the (fully parallel) Kanuk and the (hybrid) Manta architectures were proposed [17]. In [18], a synthesis approach based on motion groups was proposed and new architectures were revealed. In [19], a synthesis method based on screw theory was presented and a large number of other new architectures were discovered. One of these architectures led to the Quadrupteron [20], a partially decoupled 4-dof parallel mechanism producing the Schönflies motions.

This paper is part of an invited session that aims at benchmarking several parallel robots including the Tripteron [13], the Quadrupteron [20], the Triglide [21], the Orthoglide [22], the Hexaglide [23], the H4/I4 [16] and the Gantry-Tau robot [24]. Benchmarking results will be given in this paper for the Tripteron and Quadrupteron parallel mechanisms. Before these results are presented, we first describe the kinematic architecture of parallel mechanisms of the multipteron family, including the Tripteron, the Quadrupteron and a new member of this family — the Pentapteron. The Pentapteron is a 5-dof parallel mechanism that arose from the type synthesis performed in [25].

## II. PARALLEL MECHANISMS OF THE MULTIPTERON FAMILY

The three parallel mechanisms discussed in this paper are part of a family of parallel mechanisms that can be referred to as the multipteron family. They are based on fixed linear actuators that are used to drive a common platform with 3, 4 or 5 dofs.

### A. The Tripteron

The first member of the multipteron family, the Tripteron [13], [26], is a fully decoupled [27] 3-dof translational parallel mechanism. It is represented schematically in Fig. 1. It

This work was supported by the Natural Sciences and Engineering Research Council of Canada (NSERC) as well as by the Canada Research Chair Program.

The authors are with the Department of Mechanical Engineering, Université Laval, Québec, Québec, Canada, G1K 7P4 gosselin@gmc.ulaval.ca

[1] For a complete list of the references on the type synthesis of translational parallel mechanisms, see [12].

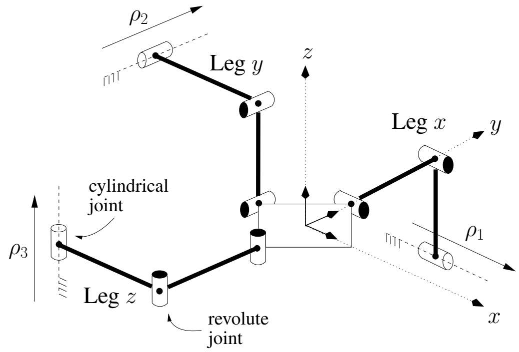


(a) Kinematic diagram.

(b) The prototype.

Fig. 1. The Tripteron: a 3-dof translational parallel mechanism.

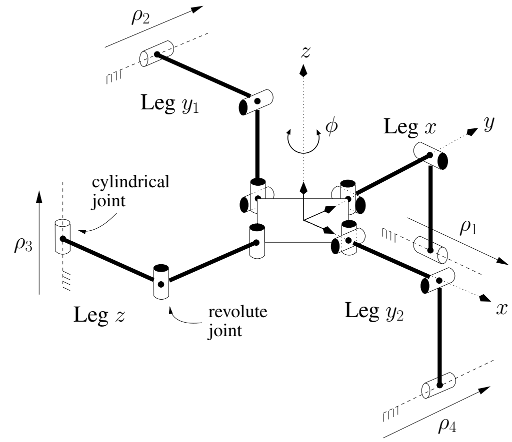


(a) Kinematic diagram.

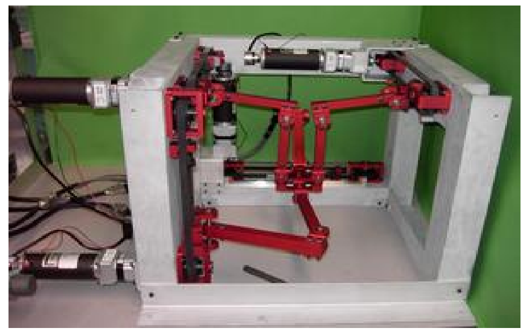

(b) The prototype.

Fig. 2. The Quadrupteron: a 4-dof Schönflies-motion parallel mechanism.

consists of three legs of the PRRR type attached orthogonally to a common platform. In each leg, the direction of the P (prismatic) joint and the axes of the R (revolute) joints are all parallel. Each of the linear actuators thereby controls one of the translations and the mechanism is fully decoupled. The kinematics and workspace of the Tripteron were presented in [13], its design was discussed in [26].

From [13], [26], the inverse (or direct!) kinematic problem of the Tripteron can be written as

$$\rho_1 = x, \quad \rho_2 = y, \quad \rho_3 = z, \tag{1}$$

where $\rho_1$, $\rho_2$ and $\rho_3$ denote the actuated joint coordinates (linear displacement of the actuators), and $x$, $y$ and $z$ denote the Cartesian coordinates of the moving platform.

### *B. The Quadrupteron*

The Quadrupteron [20], represented schematically in Fig. 2, is a 4-dof parallel mechanism capable of producing the Schönflies motions, namely all translations plus one rotation about a given fixed direction. The Quadrupteron is composed of 4 legs of the PRRU type attached to a common platform. Here, U stands for universal joints. The four fixed linear actuators are mounted along three orthogonal directions. In one of the legs, the last U joint degenerates into an R joint because of the kinematic arrangement chosen. Thus, there are three legs each having four R joints and one leg having three R joints. In each leg, the axes of the first three R joints (starting from the base) are parallel to the direction of the P joint (linear actuator) within the same leg. The axes of the R joints on the moving platform are all parallel.

The mechanism is partially decoupled since the translation along the direction of allowed rotation is controlled independently by one of the actuators. Additionally, for a constant orientation of the platform, the mechanism is fully decoupled. The kinematics, workspace and singularity analysis of the Quadrupteron were presented in [20].

Let $\rho_1$, $\rho_2$, $\rho_3$ and $\rho_4$ denote the actuated joint coordinates and $x$, $y$, $z$ and $\phi$ denote the Cartesian coordinates of the moving platform. The inverse kinematic problem of the Quadrupteron can be written as [20]

$$\rho_1 = x + s_{x1}\cos\phi - s_{y1}\sin\phi - r_{x1}, \tag{2}$$
$$\rho_2 = y + s_{x2}\sin\phi + s_{y2}\cos\phi - r_{y2}, \tag{3}$$
$$\rho_3 = z + s_{z3} - r_{z3}, \tag{4}$$
$$\rho_4 = y + s_{x4}\sin\phi + s_{y4}\cos\phi - r_{y4}, \tag{5}$$

where $s_{xi}$ and $s_{yi}$ are the coordinates of the attachment points of the legs on the platform in the coordinate frame fixed on the moving platform, while $r_{xi}$, $r_{yi}$ and $r_{zi}$ are the coordinates of the attachment points of the legs to the base expressed in the fixed coordinate frame.

The forward kinematic problem can be resolved by solving a quadratic univariate equation. There are two sets of solutions to the forward kinematic problem.

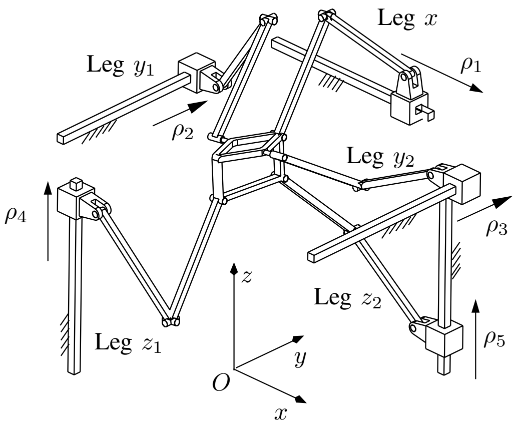


Fig. 3. The Pentapteron: a 5-dof 3T2R parallel mechanism.

### C. The Pentapteron

The Pentapteron is a 5-dof parallel mechanism that can be used to produce all translations and two independent rotations of the end-effector. Its architecture, obtained from the type synthesis presented in [25], is depicted in Fig. 3. It consists of 5 legs of the PRRRR type connecting the base to a common platform. Similarly to the Tripteron and Quadrupteron, the motion is produced by the 5 fixed linear actuators, which are mounted along three orthogonal directions. Although all legs are of the same type, their geometry varies slightly. Indeed, the geometric characteristics of the mechanism are as follows: $i)$ the five R joints attached to the platform (the last R joint in each of the legs) have parallel axes, $ii)$ the five R joints attached to the first sliding body of each leg have parallel axes, $iii)$ the first two R joints of each leg have parallel axes and $iv)$ the last two R joints of each leg have parallel axes. Also, for simplicity, the second and third R joints in each leg are built with intersecting and perpendicular axes and can thus be assimilated to a U joint. In addition, the axes of the first R joints in all the legs are arranged to be parallel to the direction of a group of two of the linear actuated joints. Therefore, two types of kinematic arrangements are possible for the legs: a) the parallel type (see legs $y_1$ and $y_2$ in Fig. 3) in which the direction of the P joint in a leg is parallel to the axis of its adjacent R joint, and b) the perpendicular type (see legs $x$, $z_1$ and $z_2$ in Fig. 3) in which the direction of the P joint in a leg is perpendicular to the axis of its adjacent R joint.

In the Pentapteron, the axes of all the R joints are always parallel to a plane. Thus, the constrained rotational dof is in a direction perpendicular to the axes of all the R joints. The position of the moving platform can be represented by $x$, $y$ and $z$ while its orientation can be represented by $\theta_x$ and $\theta_y$. The orientation ($\theta_x$, $\theta_y$) is achieved by first rotating the moving platform about the $x$-axis by $\theta_x$ and then rotating it about the $y$-axis by $\theta_y$ starting from an initial orientation, in which the axes of the R joints on the moving platform are parallel to the $x$-axis.

The inverse kinematic problem of the Pentapteron is rather simple. There are usually four solutions for the inverse kinematic problem in each of the legs (four working modes). The inverse kinematic analysis of the leg of the parallel type is equivalent to the inverse kinematic analysis analysis of a translational parallel mechanism presented in [28], [29]. A detailed discussion of the inverse kinematic problem of the Pentapteron will be presented in an upcoming publication. However, the forward kinematic problem of the Pentapteron is rather complex and is still under investigation.

TABLE I
LINK LENGTHS OF THE TRIPTERON AND QUADRUPTERON.

| Manipulator | Leg | Link length (mm) | |
|---|---|---|---|
| | | Proximal | Distal |
| Tripteron | $x$ | 247.5 | 223.0 |
| | $y$ | 237.6 | 203.0 |
| | $z$ | 272.4 | 258.0 |
| Quadrupteron | $x$ | 167.0 | 167.0 |
| | $y_1$ | 154.0 | 161.0 |
| | $y_2$ | 154.0 | 161.0 |
| | $z$ | 203.0 | 223.0 |

## III. BENCHMARKING AND EXPERIMENTAL CHARACTERISATION OF THE TRIPTERON AND QUADRUPTERON

One of the objectives of the session in which this paper is included is to compare different parallel mechanisms. Therefore, a series of properties, discussed below, have been agreed upon and will constitute the basis of this comparison. Because the development of the Pentapteron is far less advanced than that of the Tripteron and Quadrupteron, only the latter two mechanisms will be treated in this section. Moreover, since prototypes of the Tripteron (Fig. 1(b)) and the Quadrupteron (Fig. 2(b)) are available, it was decided to proceed with experimental measurements rather than to base the benchmarking on computer simulations. Although the sections of the links used in the prototypes may differ from the standard sections proposed for benchmarking, the experimental results will nevertheless provide valuable information that can then be extrapolated to different link sections if desired.

### A. Dimensions of the links

Rectangular or square aluminium tubing was used for the links of the Tripteron and Quadrupteron. For the Tripteron, the proximal links are made of tubes of $38.1mm \times 25.4mm$ having a thickness of $3.18mm$ while the distal links are made of tubes having a section of $25.4mm \times 25.4mm$ with a thickness of $1.59mm$. For the Quadrupteron, all links are made of square tubes of $19.05mm$ side having a thickness of $1.59mm$ except for the proximal link of the leg with a vertical linear actuator, which is made of a square tube of $25.4mm$ side having a thickness of $3.18mm$. The lengths of the proximal and the distal links are given in Table I for both prototypes.

### B. Workspace to Installation Space Ratio

Referring to Figs. 1 and 2, it is clearly seen that the Tripteron and Quadrupteron form a "box" around the

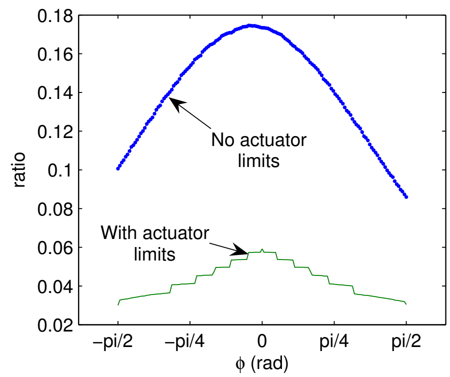


Fig. 4. Ratio of the volume of the workspace to the volume of the installation space as a function of the orientation $\phi$ for the Quadrupteron.

workspace. Therefore, for the Tripteron, the workspace to installation space ratio is strictly dependent on the ratio between the range of motion of the linear actuators and the corresponding sizes of this box. For instance, if the range of motion of the linear actuators is one half of the corresponding edge of the box, the volume of the workspace will be $(\frac{1}{2})^3 = \frac{1}{8}$. In practice, the prototype of the Tripteron was not optimized for compactness and has a lower workspace to installation space ratio. Indeed, the belt driven linear actuators have a range of motion of $250mm$ while the installation space is $776.5mm$ by $733.6mm$ by $653mm$. The workspace to installation space ratio of the prototype is then:

$$Ratio = \frac{(250mm)^3}{776.5 \times 733.6 \times 653mm^3} = 0.042 < \frac{1}{8}. \qquad (6)$$

The workspace to installation space ratio of the Quadrupteron depends on the orientation ($\phi$) of the platform. Fig. 4 illustrates the relationship between this ratio and the orientation. The first curve represents the ideal case for which the motion range of the linear actuators is equal to the edge of the installation space while the second curve corresponds to the actual prototype, which has an installation space of $0.59m \times 0.62m \times 0.49m$ $(0.18m^3)$. One interesting feature is that the maximum workspace is reached when the platform is in its reference orientation ($\phi = 0$).

### C. Cartesian Stiffness

The stiffness of the two prototypes was determined experimentally using a 6-axis force/torque sensor and displacement measurements. The measurements were repeated at several points in the workspace and the results are compiled in Table II.

### D. Natural Frequencies

The lowest natural frequency of the prototypes was determined experimentally using an accelerometer and a dynamic signal analyzer. The procedure was repeated for several configurations within the workspace. These configurations included the reference configuration (centre of the workspace) as well as configurations in which the legs were all folded or all extended. The results are given in Table III. It can be observed that the natural frequencies are somewhat lower than what would be intuitively expected. This is due to the decoupling of the mechanism: a load applied to the platform in a given Cartesian direction is essentially taken by only one of the legs.

TABLE II
MINIMUM, MAXIMUM AND AVERAGE STIFFNESS OF THE TRIPTERON AND QUADRUPTERON.

| Manipulator | Axis | Stiffness (N/m) | | |
|---|---|---|---|---|
| | | Min | Max | Average |
| Tripteron | $x$ | 19253 | 46060 | 25895 |
| | $y$ | 23297 | 46178 | 30593 |
| | $z$ | 14821 | 30556 | 18696 |
| Quadrupteron | x | 11501 | 36743 | 15147 |
| | $y$ | 21024 | 54243 | 37620 |
| | $z$ | 10176 | 27282 | 15437 |

TABLE III
MINIMUM, MAXIMUM AND AVERAGE FIRST NATURAL FREQUENCY OF THE TRIPTERON AND QUADRUPTERON.

| Manipulator | Axis | Lowest Natural Frequency (Hz) | | |
|---|---|---|---|---|
| | | Min | Max | Average |
| Tripteron | $z$ | 14.7 | 17.7 | 16.3 |
| Quadrupteron | | 14.5 | 16.8 | 15.4 |

### E. Singularity measures

As shown in [13] and [20], the Tripteron and Quadrupteron do not suffer from any constraint singularities. Indeed, the constraints applied by the legs to the platform can never become dependent.

Differentiating (1) with respect to time, we obtain the input-output velocity equation of the Tripteron

$$\dot{\rho}_1 = \dot{x}, \quad \dot{\rho}_2 = \dot{y}, \quad \dot{\rho}_3 = \dot{z}. \qquad (7)$$

It can be observed from (7) that the Jacobian matrix of the Tripteron is the identity matrix. Therefore, the robot is completely decoupled and *globally* isotropic (isotropic in all its configurations) and its kinematic dexterity is perfect everywhere in the workspace. It can also be guaranteed that there will never be any singularity inside the workspace, for any set of design parameters. Singularities of type I will occur only at the boundaries of the workspace, i.e., either when one of the linear actuators reaches one of its limits or when one of the legs is fully extended or folded. In the prototype, the geometric parameters have been chosen in order to ensure that the legs can never be fully extended or folded and the workspace is solely limited by the range of motion of the linear actuators (the workspace is a parallelepiped).

For the Quadrupteron, the Cartesian and joint velocity vectors are defined as

$$\mathbf{t} = [\dot{x}\, \dot{y}\, \dot{z}\, \dot{\phi}]^T, \quad \dot{\boldsymbol{\rho}} = [\dot{\rho}_1\, \dot{\rho}_2\, \dot{\rho}_3\, \dot{\rho}_4]^T, \qquad (8)$$

and the velocity equation can be obtained by differentiating (2)–(5) with respect to time[20]

$$\mathbf{J}\mathbf{t} = \dot{\boldsymbol{\rho}}, \qquad (9)$$

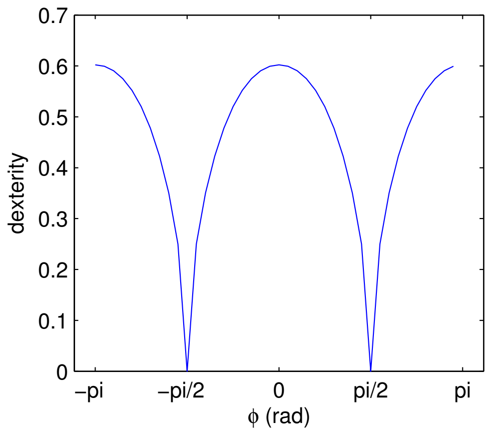


Fig. 5. Kinematic dexterity as a function of the orientation $\phi$ for the Quadrupteron.

where the Jacobian matrix $\mathbf{J}$ is defined as

$$\mathbf{J} = \begin{bmatrix} 1 & 0 & 0 & (-s_{x1}\sin\phi - s_{y1}\cos\phi) \\ 0 & 1 & 0 & (s_{x2}\cos\phi - s_{y2}\sin\phi) \\ 0 & 0 & 1 & 0 \\ 0 & 1 & 0 & (s_{x4}\cos\phi - s_{y4}\sin\phi) \end{bmatrix}. \quad (10)$$

Since the Jacobian matrix is independent from the position coordinates and depends only on the angle $\phi$, the dexterity is constant throughout the workspace for a given value of $\phi$. Therefore, singularities will occur only for specific values of $\phi$. This condition is obtained by setting the determinant of $\mathbf{J}$ to zero, which leads to

$$\tan\phi = \frac{s_{x2} - s_{x4}}{s_{y2} - s_{y4}}. \quad (11)$$

The solutions of this equation are the two following values: $\pm\frac{\pi}{2}$. For any other orientation of the effector, the workspace is free of singularities. This is clearly illustrated in Fig. 5, where the dexterity of the mechanism is plotted as a function of the orientation $\phi$. By limiting the orientation of the platform between $-\pi/2$ and $\pi/2$, the Quadrupteron is singularity free and its kinematic dexterity is as shown in Fig. 5.

### F. Kinematic sensitivity

Referring to (1), it is clear that the inverse and direct kinematics of the Tripteron are independent from the link lengths. Therefore, the Tripteron is completely insensitive to errors in the link lengths. In fact, such errors will affect the coordinates of the passive revolute joints but not the position of the platform.

From (2)–(5), it is clear that the inverse and direct kinematic problems of the Quadrupteron are independent from the link lengths. Therefore, the Quadrupteron is completely insensitive to errors in the link lengths. Similarly to the case of the Tripteron, errors in these lengths will only affect the passive revolute joints but not the position and orientation of the platform.

TABLE IV

MAXIMUM ACCELERATIONS PERFORMED BY THE PROTOTYPES.

| Manipulator | Maximum acceleration |
|---|---|
| Tripteron | 8.64 g |
| Quadrupteron | 5.19 g |

### G. Maximum accelerations

*1) Trajectory:* The maximum acceleration for each of the prototypes was obtained by generating a simultaneous trajectory at each of the actuators. The trajectory is based on a fifth order polynomial that ensures continuity of velocities and accelerations, namely

$$s(\tau) = \Delta p(6\tau^5 - 15\tau^4 + 10\tau^3), \quad (12)$$

with

$$\tau = \frac{t}{T}, \quad (13)$$

where $t$ is the time, $T$ is the total duration of the trajectory, and $\Delta p$ is the magnitude of the total displacement performed during the trajectory. Differentiating (12) twice with respect to time, it is easy to show that $T$ can be adjusted in order to obtain a prescribed maximum acceleration $a_{\max}$. The derivation leads to:

$$T = \sqrt{\frac{10\sqrt{3}}{3a_{\max}}|\Delta p|}. \quad (14)$$

*2) Measurements:* Since the second order derivative of the encoders of the prototype is very noisy, an indirect measurement of the acceleration was used instead. The maximum acceleration was computed from the fastest prescribed trajectory which can be produced without saturation of the actuators. A verification was also carried out by comparing the plots of the actual position of the encoder with the prescribed one, in order to ensure that the manipulator followed the prescribed trajectory closely. Fig. 6 shows an example of this comparison between the ideal trajectory and the actual one. The maximum accelerations obtained experimentally for the two prototypes are given in Table IV, where $g$ stands for the gravitational acceleration.

## IV. CONCLUSION

This paper discussed several properties of parallel mechanisms of the multipteron family. First, the kinematic architectures of the multipteron family were presented. In addition to the Tripteron (3-dof) and the Quadrupteron (4-dof), a new mechanism, the Pentapteron, was introduced. The Pentapteron is a 5-dof mechanism that can be used in applications where a 3T2R motion pattern is required. Then, the Tripteron (3-dof) and Quadrupteron (4-dof) were revisited. Several of their properties were highlighted and measurements were performed on the prototypes in order to assess some of their characteristics. One of the key features of the Tripteron and Quadrupteron robots is that their kinematics is extremely simple, which leads to ideal dexterity and a singularity free workspace. Their simple kinematics also leads to decoupling (or partial decoupling

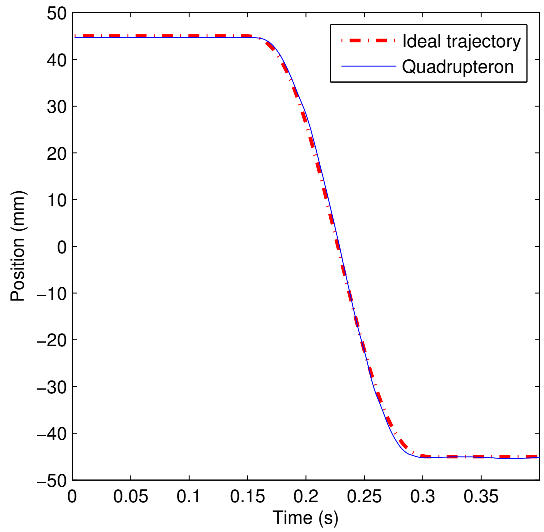


Fig. 6. Example of a trajectory used to obtain the maximum acceleration of the two robots.

for the Quadrupteron) and makes these robots insensitive to errors in the link lengths. Finally, it was shown that the prototypes built can perform accelerations of approximately 8 g and 5 g respectively.

## REFERENCES

[1] I.A. Bonev, "Delta Robot — the Story of Success," *The Parallel Mechanisms Information Center*, online article (http://www.parallemic.org/Reviews/Review002.html), May 2001.

[2] H. Makino and N. Furuya, "SCARA Robot and its Family," *Proceedings of the International Conference on Assembly Automation*, 1982, pp. 433–444.

[3] R. Clavel, "Device for the Movement and Positioning of an Element in Space," US Patent No. 4,976,582, 1990.

[4] W.T. Appleberry, "Anti-Rotation Positioning Mechanism," US Patent No. 5,156,062, 1992.

[5] R. Di Gregorio, and V. Parenti-Castelli, "A Translational 3-DOF Parallel Manipulator," *Advances in Robot Kinematics: Analysis and Control*, J. Lenarcic and M. L. Husty, eds., Kluwer Academic Publishers, pp. 49–58, 1998.

[6] L.-W. Tsai, "The Enumeration of a Class of Three-DOF Parallel Manipulators," *Proceedings of the Tenth World Congress on the Theory of Machines and Mechanisms*, Oulu, Finland, Vol. 3, pp. 1121–1126, 1999.

[7] J.M. Hervé, "Dispositif pour le Déplacement en Translation Spatiale d'un Élément dans l'Espace en Particulier pour Robot Mécanique," European Patent No. 0 494 565 A1, 1992.

[8] J.M. Hervé and F. Spatacino, "Structural Synthesis of Parallel Robots Generating Spatial Translation," *Proceedings of the Fifth International Conference on Advanced Robotics*, Pisa, Italy, Vol. 1, pp. 808–813, 1991.

[9] J.M. Hervé, "Design of Parallel Manipulators via the Displacement Group," *Proceedings of the Ninth Congress on the Theory of Machines and Mechanisms*, Pisa, Italy, Vol. 1, pp. 808–813, 1995.

[10] A. Frisoli, D. Checcacci, F. Salsedo, and M. Bergamasco, "Synthesis by Screw Algebra of Translating In-Parallel Actuators Mechanisms," *Advances in Robot Kinematics*, J. Lenarcic and M. M. Stanisic, eds., Kluwer Academic Publishers, pp. 433–440, 2000.

[11] X. Kong and C.M. Gosselin, "Generation of Parallel Manipulators With Three Translational Degrees of Freedom Based on Screw Theory," *Proceedings of the 2001 CCToMM Symposium on Mechanisms, Machines, and Mechatronics*, Saint-Hubert, QC, Canada, 2001.

[12] X. Kong and C.M. Gosselin, "Type synthesis of 3-DOF translational parallel manipulators based on screw theory and a virtual joint," *Proceedings of the 15th CISM-IFToMM Symposium on Robot Design, Dynamics and Control*, Saint-Hubert, Montreal, Canada, Paper 04-06, 2004.

[13] X. Kong and C.M. Gosselin, "Kinematics and Singularity Analysis of a Novel Type of 3-CRR 3-DOF Translational Parallel Manipulator," *The International Journal of Robotics Research*, Vol. 21, No. 9, September, 2002, pp. 791–798.

[14] J. Angeles, A. Morozov, and O. Navarro, "A Novel Manipulator Architecture for the Production of SCARA motions," *Proceedings of the IEEE International Conference on Robotics and Automation*, April 24-28, San Francisco, 2000, pp. 2370-2375.

[15] J. Angeles, "The Morphology Design for a Parallel Schönflies-motion Generator," *Proceedings of the Second International Colloquium on Robotic Systems for Handling and Assembly*, May 10–11, Braunschweig, Germany, 2005, pp. 37–56.

[16] F. Pierrot, F. Marquet, O. Company and T. Gil, "H4 Parallel Robot: Modeling, Design and Preliminary Experiments," *Proceedings of the 2001 IEEE International Conference on Robotics and Automation*, May 21–26, Seoul, Korea, 2001, pp. 3256–3261.

[17] L. Rolland, "The Manta and the Kanuk: Novel 4-DOF Parallel Mechanisms for Industrial Handling," *Proceedings of the ASME Dynamic Systems and Control Division, IMECE'99 Conference*, Nov. 14-19, Nashville, USA, Vol. 67, 1999, pp. 831-844.

[18] J. Angeles, "The Qualitative Synthesis of Parallel Manipulators," *Proceedings of the Fundamental Issues and Future Research Directions for Parallel Mechanisms and Manipulators Workshop*, October 2-4, Quebec City, 2002, pp. 159–169.

[19] X. Kong and C.M. Gosselin, "Type Synthesis of 3T1R 4-DOF Parallel Manipulators Based on Screw Theory," *IEEE Transactions on Robotics and Automation*, April, Vol. 20(2), pp. 181–190, 2004.

[20] P.-L. Richard, C.M. Gosselin and X. Kong, "Kinematic Analysis and Prototyping of a Partially Decoupled 4-DOF 3T1R Parallel Manipulator," *Proceedings of the 2006 ASME Design Engineering Technical Conferences & Computers and Information in Engineering Conference*, Philadelphia, USA, September 10–13, 2006.

[21] J. Hesselbach and G. Pokar, "A Class of New Robots for Micro-Assembly," *Production Engineering*, Vol. 7, No. 1, 2000, pp. 113–116.

[22] D. Chablat and P. Wenger, "Architecture Optimization of a 3-DOF Translational Parallel Mechanism for Machining Applications, the orthoglide," *IEEE Transactions on Robotics and Automation*, Vol.19, no.3, 2003, pp. 403- 410.

[23] S. Weikert, "Beitrag zur Analyse des dynamischen Verhaltens von Werkzeugmaschinen," Diss. Technische Wissenschaften ETH Zrich, Nr. 13596, 2000.

[24] L. Johannesson, V. Berbyuk and T. Brogardh, "Gantry-Tau: A New Three Degrees of Freedom Parallel Kinematic Robot," *Proceedings of the Mekatronikmöte2003*, August 27-28, Göteborg, Sweden, 2003, pp. 1–6.

[25] X. Kong and C.M. Gosselin, "Type Synthesis of 5-DOF Parallel Manipulators Based on Screw Theory," *Journal of Robotic Systems*, Vol. 22, No. 10, 2005, pp. 535–547.

[26] C.M. Gosselin, X. Kong, S. Foucault and I. Bonev, "A Fully Decoupled 3-dof Translational Parallel Mechanism," *Proceedings of the 4th Chemnitz Parallel Kinematics Seminar / 2004 Parallel Kinematic Machines International Conference*, 2004, pp. 595–610.

[27] X. Kong and C.M. Gosselin, "Type Synthesis of Input-Output Decoupled Parallel Manipulators," *Transactions of the Canadian Society for Mechanical Engineering*, Vol. 28, No. 2A, 2004, pp. 185–196.

[28] X. Kong and C.M. Gosselin, "Discussion: 'Kinematics of the Translational 3-URC Mechanism' [Di Gregorio, R., 2004, ASME J. Mech. Des., 126, pp. 1113–1117]," *ASME Journal of Mechanical Design*, Vol. 128(4), pp. 812–813, 2006.

[29] R. Di Gregorio, "Closure to "Discussion of 'Kinematics of the Translational 3-URC Mechanism' " (2006, ASME J. Mech. Des., 128, pp. 812–813)," *ASME Journal of Mechanical Design*, Vol. 128(4), pp. 814, 2006.